Bending elastic moduli of lipid bilayers : modulation by solutes

H.P. Duwe, J. Kaes, E. Sackmann

J. Phys. France **51** (1990) 945-962 15 MAI **1990,** PAGE 945

Classification
Physics Abstracts
87.22F

Bending elastic moduli of lipid bilayers : modulation by solutes

H. P. Duwe, J. Kaes and E. Sackmann

Physik-Department, Biophysics Group, Technische Universität München, D-8046 Garching, F.R.G.

(*Reçu le 12 septembre 1989, révisé le 5 janvier 1990, accepté le 31 janvier 1990*)

Abstract. — We present high precision measurements of the bending elastic moduli for bilayers of a variety of different lipids and of modifications of the flexural rigidity by solutes. The measurements are based on the Fourier analysis of thermally excited membrane undulations (vesicle shape fluctuations) using a recently developed dynamic image processing method. Measurements of the bending modulus as a function of the undulation wave vector provide information on the limitation of the excitations by the constraint of finite membrane area (surface tension effects) and by transient lateral tensions arising in each monolayer by restricted diffusion at high wavevectors. Measurements of the autocorrelation function of the undulation amplitudes provide a further test of the theoretical models. Studies of the effect of solutes show that cholesterol increases the bending modulus of dimyristoylphosphatidylcholine from $K_c = 1.1 \times 10^{-12}$ ergs to 4.2×10^{-12} ergs (at 30 mole %). Incorporation of about 2 mole % of a short bipolar lipid reduces K_c to the order of kT. A scaling law between the projected radius of gyration, R_g, of these hyperelastic vesicles and the surface area, A (or number of lipid molecules N) of $R_g^2 \propto A^{0.94 \pm 0.02}$ was established.

1. Introduction.

Lipid bilayer vesicles fascinate physicists because of their peculiar elastic and dynamic properties which are dominated by a very soft bending elastic modulus on the order of 10 kT [1-4]. They appeal to biophysicists since (despite their simple structure) they exhibit typical mechanical and rheological features of cell membranes. The bending elastic modulus may be lowered by solutes towards the thermal energy in order to approach the limit of random surfaces. New fascinating phenomena arise in mixed bilayers where the coupling of lateral phase separation and curvature effects lead to a manifold of metastable vesicle shapes [8]. By using dynamic image processing methods, it has become possible to determine the mean square amplitudes and the correlation times of the thermal membrane excitations as a function of the wavevector in the optical regime, thus allowing high precision measurements of the bending elastic modulus. In the present work we present first a more detailed description of our experimental procedure of evaluation of the membrane undulations [1]. Secondly, we summarize our recent measurements of the bending elastic moduli of various lipid bilayers and demonstrate that the method is well suited to distinguish vesicles composed of different numbers of bilayers. In a third part we present measurements of the

autocorrelation function of the membrane excitations and show that the equilibrium and the dynamic models of the vesicle fluctuations [6, 7] agree well with experimental data. Finally, we present measurements of the radius of gyration of vesicles with bending elastic moduli of the order of kT as function of the total surface area and establish a scaling law with broken exponent.

2. Theoretical background of the method.

It is generally accepted now that the thermal undulations of vesicles and also biconcave (and moderately swollen) erythrocytes can be described in terms of the quasi-spherical model first worked out by Helfrich [4] and Schneider [5] and subsequently improved by Peterson [6] and Milner and Safran [7] to include spontaneous curvature effects and to account for the suppression of long wavelength modes [1] by the constraint of constant area. The thermal excitations of quasi-spherical vesicles are described in terms of a spherical harmonics expansion ($y_{\ell m}(\vartheta, \varphi)$) of the middle surface separating the two monolayers. The latter is determined by the radius $r(\vartheta, \varphi)$ (ϑ: polar angle, φ azimuthal angle) which is

$$r(\vartheta, \varphi, t) = r_0 \left(1 + \sum_{\substack{m=0 \\ \ell=2}}^{\infty} a_{\ell,m}(t)\, Y_{\ell,m}(\vartheta, \varphi) \right) \tag{1}$$

where r_0 is the so called equivalent radius. It is equal to the radius of a sphere of the same volume, V, as the vesicle. For symmetric bilayers, where spontaneous curvature effects can be ignored, the undulations are determined by the elastic energy.

$$E_c = \int_A \left(\frac{1}{2} K_c H^2 + \gamma \right) \mathrm{d}A \tag{2}$$

where H is the mean curvature: $H = 1/r_1 + 1/r_2$ (r_1, r_2: principal radii of curvature), K_c is the bending elastic modulus and A is the surface area of the vesicle. γ is a Lagrange multiplier which accounts for the constraint of constant area. Physically it corresponds to the lateral tension which arises for those excitational modes that require a larger excess area than available. Provided the excitation of the spherical harmonic modes follows the equipartition theorem, the normalized mean square amplitudes of the spherical harmonic mode characterized by the angular momentum (ℓ) and magnetic quantum number (m) are given by

$$\left\langle |a_{\ell,m}|^2 \right\rangle = \frac{r_0^2 K_B T}{K_c(\ell+2)(\ell-1)[\ell(\ell+1) - \tilde{\gamma}]} \tag{3}$$

where $\tilde{\gamma} = \gamma r_0^2 / K_c$. As pointed out first by Brochard and Lennon [9], the damping of the membrane bending undulations is determined by the hydrodynamic flow of the enclosed and surrounding fluid and for that reason the modes are completely overdamped. The (temporal) autocorrelation function of the amplitude $a_{\ell m}(t)$ are exponentials [6, 7]

$$\langle a_{\ell,m}(t)\, a_{\ell,m}(0) \rangle = \left\langle |a_{\ell,m}|^2 \right\rangle \exp\{-\omega_{\ell,m}\, t\} \tag{4}$$

where

$$\omega_{\ell,m} = \frac{K_c}{\eta r_0^3} (\ell(\ell+1) - \tilde{\gamma}) / Z(\ell) \tag{5}$$

$$Z_\ell = \frac{(2\ell+1)(2\ell^2+2\ell-1)}{\ell(\ell+1)(\ell+2)(\ell-1)} \tag{6}$$

and η is the viscosity of water.

It is important to note that equipartition is possible only if the flow within the bilayer is fast enough to accomodate for local density fluctuations (in each monolayer) associated with the undulations. A break-down of the equipartition is suggested for membranes containing cholesterol (cf. Sect. 4).

Experimentally, the excitations of the vesicle have to be analysed in terms of the fluctuations of the contour observed in the phase contrast microscope. This is possible provided

1) the vesicle is quasi-spherical so that the image plane goes through its center of mass
2) the time over which the fluctuations are observed is large compared to the response (= relaxation) time of the excitations.

Let the Fourier transform of the momentaneous contour at time t be

$$r(\varphi, t) = r_0 \sum_{q=0}^{q_{\max}} v_q(t) \exp\{-iq\varphi\} \tag{7}$$

where φ is the longitudinal angle and $v(\varphi, t)$ is determined by the deviation of the vesicle surface from the sphere at $\vartheta = \pi/2$. By using equation (1) one obtains for the Fourier component $v_q(t)$ of equation (7) [1, 3]

$$v_q(t) = \frac{1}{2\pi} \sum_{\ell=q,m}^{\ell_{\max}} a_{\ell,m}(t) \int_0^{2\pi} Y_{\ell,m}\left(\frac{\pi}{2}, \varphi\right) e^{iq\varphi}\, d\varphi\,. \tag{8}$$

The sum starts at $\ell = q$ but the minimum of ℓ must be larger than two. The mean square amplitudes of the contour fluctuations are then

$$\left\langle |v_q(t)|^2 \right\rangle = \frac{k_B T r_0^2}{K_c} \sum_{\ell=q,m}^{\ell_{\max}} \left\langle |a_{\ell,m}(t)|^2 \right\rangle P_{\ell,m}^2\left(\cos\frac{\pi}{2}\right) \tag{9}$$

where $P_{\ell,q}(\cos(\pi/2))$ are the values of the Legendre Polynominals in the equatorial plane. Thus the mean square amplitudes of the fluctuation of the contour are directly related to the mean square amplitudes of the spherical harmonics given in equation (3). The sum in equation (9) converges rapidly with increasing ℓ and has been calculated for the quantum numbers $2 \leqslant q \leqslant 10$ up to $\ell = \ell_{\max} = 34$ [3].

3. Experimental procedure.

3.1 PREPARATION OF THIN WALLED VESICLES. — Giant vesicles with diameters larger than 10 μm were prepared by the following procedure. The lipid or lipid mixture was dissolved in 2 : 1 chloroform/methanol (1 mM solution). 20 μl of this solution (containing about 2×10^{-8} mole or 10^{-5} g of lipid) was distributed as a thin film on the surface of a microscope cover glass. The solvent was evaporated by placing the substrate in a vacuum chamber for a minimum of one hour. The cover glass was inserted in a sample cell (where it served as the bottom window) and was fixed with silicon grease. The sample cell was filled with distilled water or a 100 mM solution of mannit and the top closed (and sealed) with a second cover glass (the top window). The whole sample cell was inserted into a thermostated measuring chamber made of V2A steel. The temperature could be varied between 0 and 50 °C by using

Peltier elements cooled by water. The temperature in the sample chamber was measured with a Pt100 temperature sensor.

3.2 EXPERIMENTAL PROCEDURE USED FOR FOURIER ANALYSIS OF VESICLE CONTOUR FLUCTUATIONS. — The vesicles were observed and evaluated with an inverted Zeiss Axiomat microscope. It was mounted (on air cushions) on a heavy ground plate which was suspended from the laboratory ceiling to reduce vibrations caused by walking. A schematic view of the optical set-up is shown in figure 1. One advantage of the Axiomat is that the position of the image plane of the (infinity adapted) objective can be choosen freely. In this way a normal bright field objective can be used for phase contrast microscopy by placing a phase plate in the image plane far away from the objective. For the present work, a bright field air objective of magnification 50 × (Zeiss) was used. Since the working distance of the objective was only 300 μm, the vesicles near the bottom window of the sample cell had to be observed by an inverted microscope. Images of the vesicles selected were taken with a charge coupled device (CCD) camera (frame transfer camera, HR600M, Aqua-TV company, Kempten, FRG) onto which a section of 40 × 40 μm^2 of the image plane was projected. The camera is connected to an image processing system (MAXVIDEO, DataCube BOSTON, USA) with VME bus and 0S-9 operating system. With this system the images from the video camera are digitized 512 × 512 pixels and 256 gray levels.

A fast algorithm was developed which allowed us to evaluate the (time dependent) contour of a vesicle at a rate of 5-10 per second and to store the data in the computer memory. The procedure is illustrated in figure 2. Since the phase shift of the light is maximal if it passes tangential to the vesicle surface, the transient contour (that is the equator of quasi-spherical vesicle) corresponds to a sharp minimum of the brightness of the image. First a starting point (coordinate x_0, y_0) of the contour is selected by the cursor. Each pixel has 8 neighbours which define 8 directions (numbered 0 to 7 in Fig. 2). As second step the adjacent contour point is searched as follows : the intensity over three bands comprising 46 pixels and laying in three different directions of the eight are summed. The position of the contour (x_1, y_1) adjoining the starting point (x_0, y_0) lies in the direction of minimum total intensity and is given by ($x_0 + 1$, $y_0 + 1$). The three test directions are determined by the direction of the previous step. The above procedure is repeated until one returns to the position of the starting point. The number of 46 pixels is of arbitrary source. It has been found optimal to account for the fact that the width of the intensity valley is 5 to 6 pixels (cf. Fig. 2). After having determined (and stored) the positions of the contour the center of mass of the vesicle is determined according to

$$S_x = \frac{1}{K} \sum_{i=0}^{K-1} x_i ; \quad S_y = \frac{1}{K} \sum_{i=0}^{K-1} y_i \tag{10}$$

where K is the number of pixels of the contour and is typically K = 500-1 000. Now, the polar coordinates (φ_i, R_i) of the contour are determined with the center of mass as origin.

The Fourier decomposition of the contour is performed using a Fast Fourier Transform procedure [10]. For this procedure the contour line must be divided into 2^N equidistant points. Since the contour line is determined by 500-1 000 pixels a new set of $2^9 = 512$ points ($R_{0,511}$) is determined from the original set ($R_{i,K}$) by averaging the values lying within segments of opening angle $2\pi/128$.

The Fourier transformation yields complex Fourier coefficients

$$c_q = a_q + i b_q$$

where q runs from -255 to $+255$. Of these the values for $0 \leqslant q \leqslant 10$ are stored.

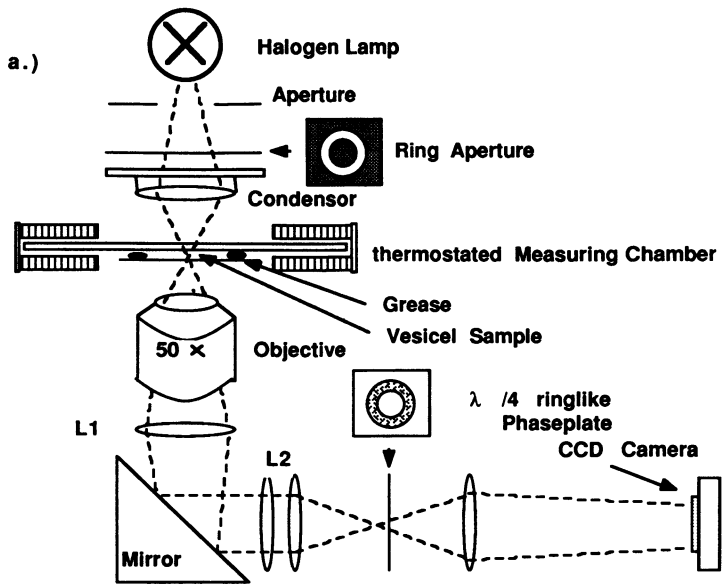

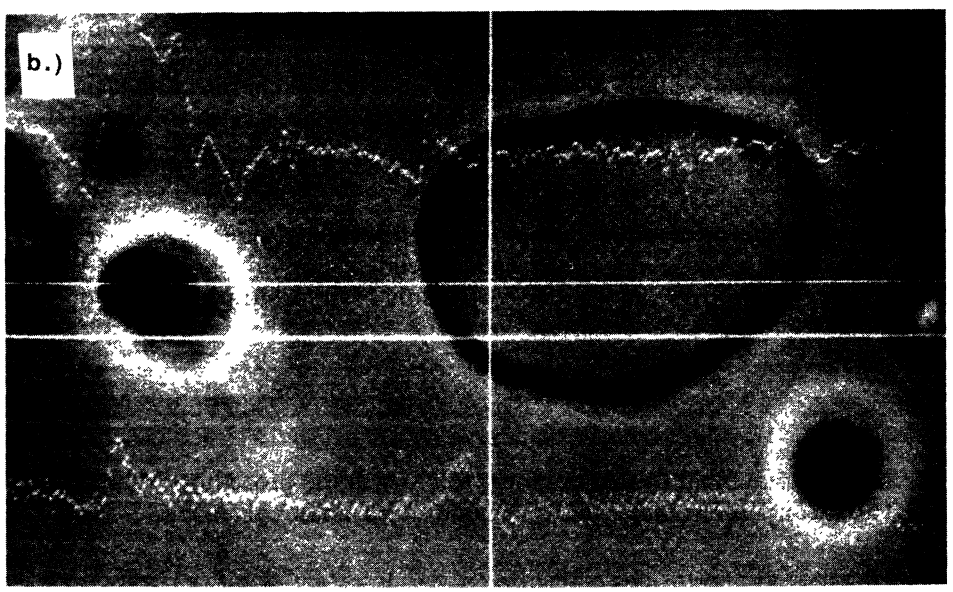

Fig. 1. — a) Schematic view of apparatus built around a inverted Zeiss Aximat microscope used for observation of vesicle. Since the focus of the objective is set at infinity its image plane can be positioned at will by using the lenses L_1 and L_2 and the mirror. Therefore a normal bright field objective (Here : Zeiss 50 ×, Air, Pol, numerical aperture 0.95, working distance 300 μm) can be used for phase contrast microscopy by placing a (ring-like) phase plate in the image plane. The sample could be illuminated with a 100 Watt halogen lamp (Zeiss) or a high pressure mercury lamp (HBO-100) with ultraviolett cut-off filter which improved the optical resolution. b) DMPC-vesicle with intensity distribution (white shaky curve) along a direction indicated by the white straight line. The positions of the contour is determined by the two minima in the intensity distribution.

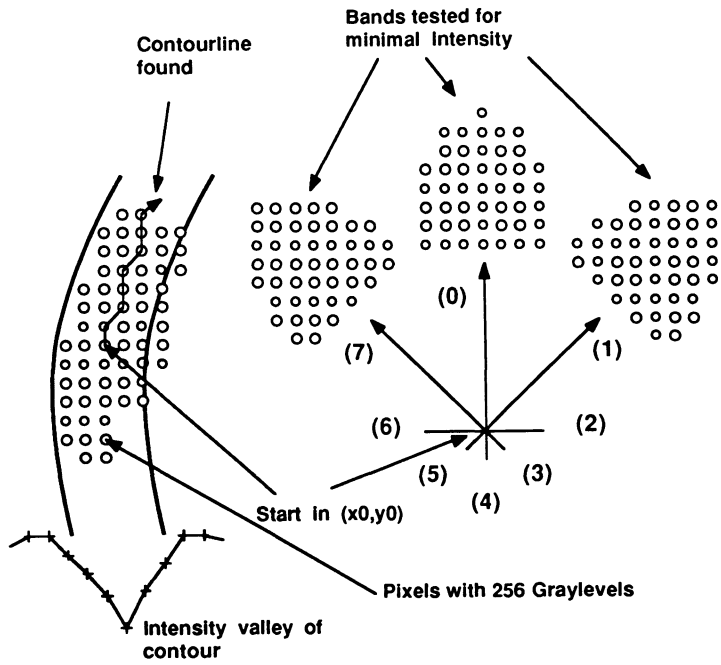

Fig. 2. — Schematic representation of algorithm used to determine the transient contour of the vesicles. The starting point at (x_0, y_0) is selected interactively the first time. Then the intensity over three bands comprising 46 pixels and lying in three different directions (of the eight possible) are summed to find the direction of minimum intensity. An example of the depth of the intensity valley is shown at the left lower corner.

As the next step, the mean square amplitude is determined as follows :

Since the excitation modes are statistically independent, the time average of the contour is determined by averaging over the Fourier coefficients of an arbitrary number of M-contours

$$\bar{C}_{n,q} = \frac{1}{M} \sum_{i=n-\frac{M}{2}}^{n+\frac{M}{2}} (a_{i,q} + i b_{i,q}) = \bar{a}_{n,q} + i \bar{b}_{n,q} \tag{11}$$

where n is an eligible number of that contour from which the procedure is started. It must be $n \geqslant M/2$. The mean square amplitudes of mode q are finally given by

$$\left\langle |V_q(t)|^2 \right\rangle = \frac{1}{N} \sum_{i=1}^{N} \left\{ (a_{i,q} - \bar{a}_{n,q})^2 + (b_{i,q} - \bar{b}_{n,q})^2 \right\} . \tag{12}$$

The bending modulus is directly obtained from equation (9). The average vesicle radius is given by

$$r_0 = \sqrt{\overline{a_{n,0}^2} + \overline{b_{n,0}^2}} \tag{13}$$

where $a_{n,0}$, $b_{n,0}$ are the averaged Fourier coefficients for $q = 0$. It should be noted that in the limit of infinitely long sampling times, the average coefficients $\bar{a}_{n,q}$ and $\bar{b}_{n,q}$ in equation (11) become zero. In the present procedure we analysed the difference between the contour

c_q at time t and the contour obtained by averaging over a time, Δt, which is considerably longer than the correlation time of the longest wavelength mode. In this way it was possible to analyse also vesicles of slightly oval form, which change shape very slowly, as predicted by Millner and Safran [7]. The values of K_c obtained for slightly oval vesicles agree well with those exhibiting a spherical shape, showing that the quasispherical model applies also to slightly oval vesicles.

4. Experimental results.

4.1 BENDING MODULI OF SYNTHETIC AND NATUREL LIPIDS AND THE EFFECT OF SOLUTES. — Figure 3 shows values of the bending modulus of DMPC bilayers as a function of the wave vector q characterizing the undulations of the contour (cf. Eq. (7)) measured at 30 °C. The K_c-value of the lowest order mode ($q = 2$) is clearly larger than that of the higher modes ($q = 3$ to 10). The latter agree within experimental error although a shallow minimum appears to exist around $q = 5$. The average value of K_c obtained for $3 \leqslant q \leqslant 10$ is $K_c = (1.15 \pm 0.15) \times 10^{-12}$ erg. It is essential to analyse a sufficiently large number of images in order to probe all excitational states of the vesicle. By attributing the apparent incrase of K_c at $q < 3$ to the influence of the surface tension, we determined values of $\tilde{\gamma}$ for the $\ell = 2$ and $\ell = 3$ modes. These values were used below in order to correct the correlation times in table II and are given there. In the present experiments, we analyzed at least 100 images in order to determine K_c from the lowest order mode ($\ell = 2$). The average value of K_c decreases with the number of contours analysed. That is the true bending elastic modulus is given by the asymptotic values of K_c.

Figure 4 shows measurements of the bending modulus, K_c, as a function of the wave vector q for DMPC containing 20 mole % and 30 mole % cholesterol. A qualitatively different q-dependence as in figure 3 is observed. As in the case of pure DMPC, the K_c-value for the lowest order mode ($q = 2$) is larger than for $q = 3$. However, at $q > 3$, K_c increases again with the wave vector. Below, this behaviour is interpreted in terms of a reduction of the high order modes by the reduced flow of the bilayer.

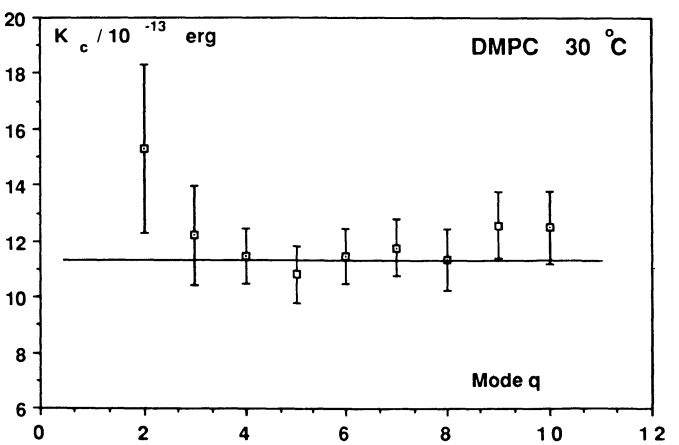

Fig. 3. — Bending elastic modulus, K_c, of (most probably) single walled vesicle of DMPC as function of wave number q characterizing the undulations of the vesicle contour. Vesicle radius $r_0 = 9.91$ μm ; temperature $T = 30$ °C ; 478 images taken at time intervals of 0.2 s were analysed.

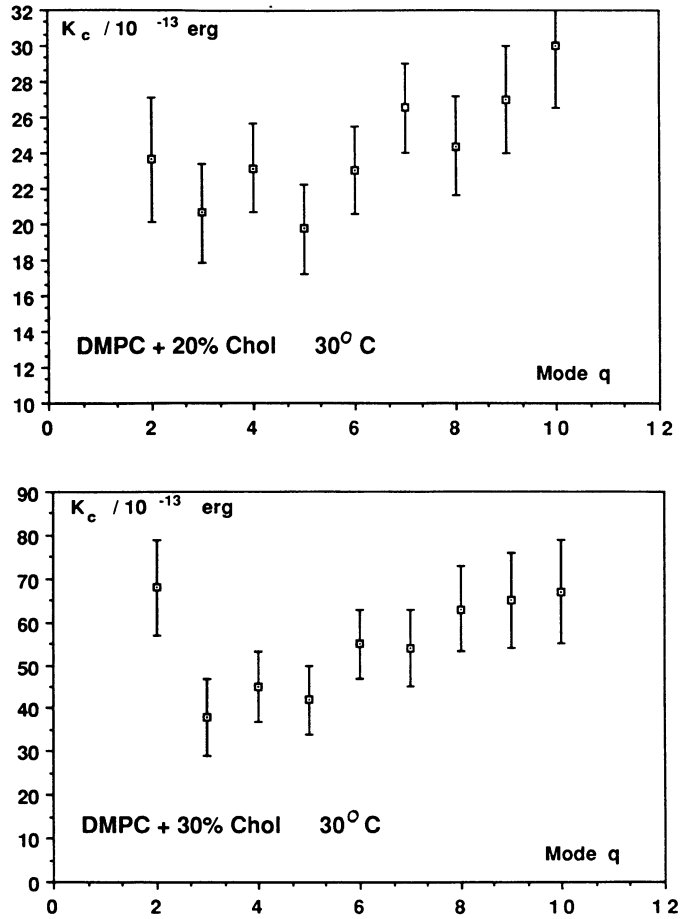

Fig. 4. — Bending elastic moduli of single walled vesicle of DMPC containing (a) 20 mole % and (b) 30 mole % cholesterol, respectively. Measuring temperature 30 °C. Case of figure 4a : 176 images taken at time intervals of 0.2 s were analysed ; vesicle radius was 9.88 μm. Case of figure 4b : 178 images taken at time intervals of 0.25 s were analysed ; vesicle radius 12.19 μm.

Figure 5 shows a summary of the average bending moduli of vesicles of DMPC. Altogether 26 vesicles were analysed. The ordinate of the histogram gives the number of cells yielding the same K_c-value. Clearly, four groups with averages of $K_c = 1.1 \times 10^{-12}$; $K_c = 2.1 \times 10^{-12}$; $K_c = 3.1 \times 10^{-12}$ and $K_c = 4.1 \times 10^{-12}$ ergs are distinguished. The larger K_c-values are multiples of the minimum value. This leads to the conclusion that these groups correspond to vesicles with shells composed of one, two, three, and four bilayers.

Figure 7 summarizes the values of the bending moduli of lipid bilayers determined in our laboratory. The two more exotic lipids 1,2 di ($5C_1$-16 : 0)-PC and galactosyldiglyceride are included in this figure. For comparison, we also give the value of K_c of erythrocytes measured by direct Fourier analysis of the membrane excitations by reflection interference contrast microscopy [11]. Each point corresponds to the measurement of one vesicle. The most remarkable results are :

1) In several cases the measured K_c-values clearly form groups. The differences between the average K_c-values of adjacent groups are equal to the lowest values of K_c. Therefore each

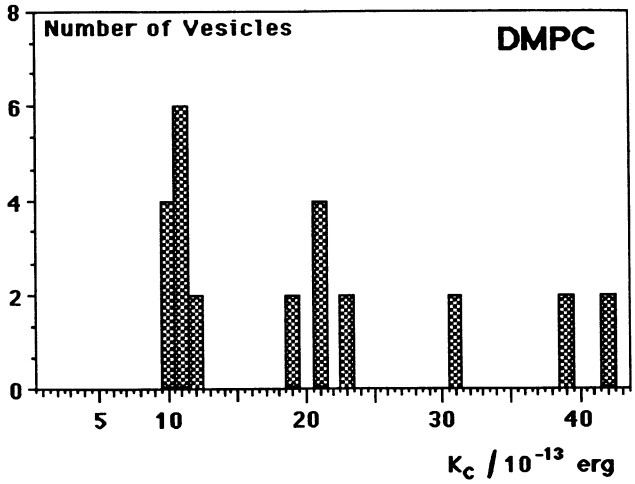

Fig. 5. — Summary of average values of K_c measured for DMPC vesicles at 30 °C. The ordinate of the histogram gives the numbers of vesicles exhibiting the same bending elastic modulus.

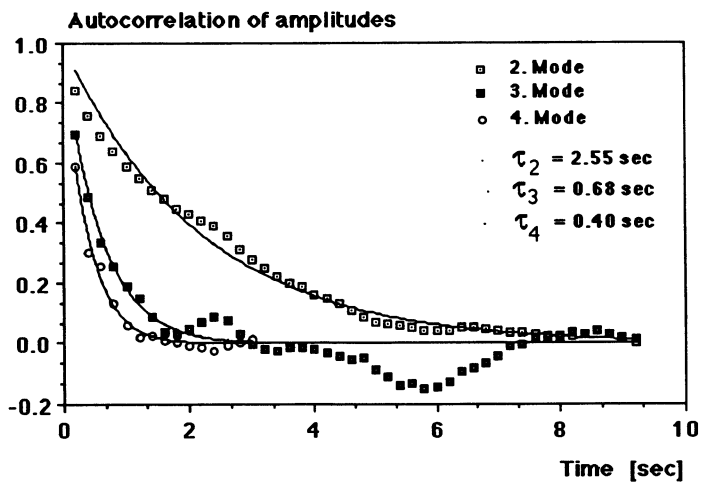

Fig. 6. — Plot of auto-correlation function $\langle v_q(t)\, v_q(0)\rangle$ of amplitudes of contour fluctuations for the three lower order modes. The data points are fitted by single exponential functions using a least square fitting procedure.

group of K_c-values corresponds to a vesicle composed of a fixed number of bilayers. The lowest values are attributed to single shell vesicles. This demonstrates the high degree of accuracy of the present technique. The average values of the bending moduli of the single shell vesicle are given in table I.

2) Cholesterol leads to a strong increase of the bending stiffness of phospholipid bilayers. This corresponds well with the strong increase of the lateral area compressibility modulus caused by cholesterol [13].

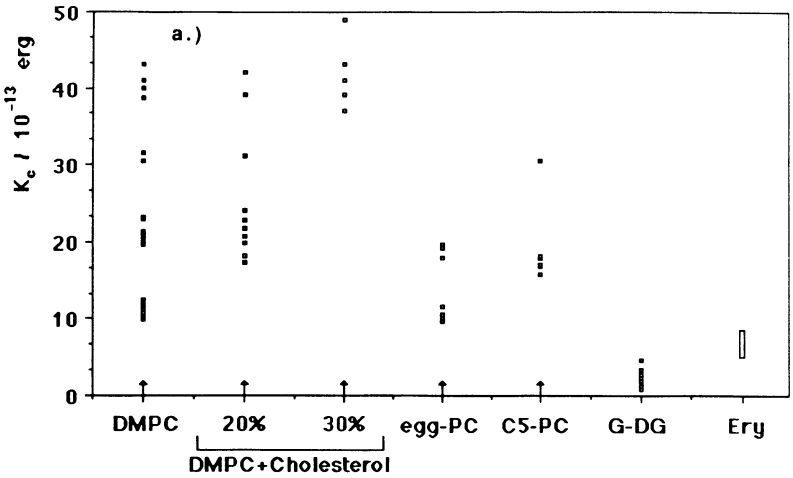

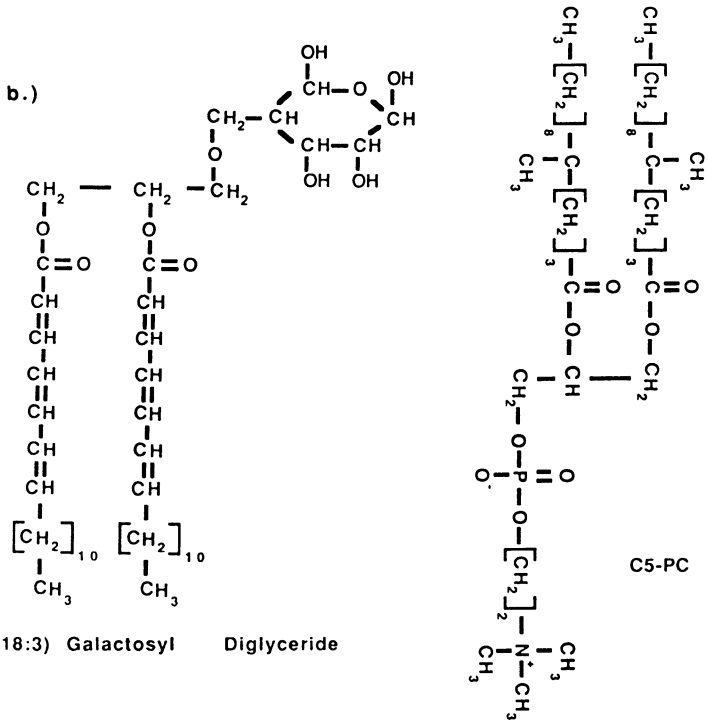

Fig. 7. — a) Summary of bending elastic moduli, K_c, of vesicles of various synthetic and natural lipids and of DMPC-cholesterol mixtures. On the right side the value of red blood cell membrane is shown. The lipid C5-PC is a phosphatidylcholine (PC) with a branched chain. G-DG (= galactosyldiglyceride) is a plant cell lipid with a high content of $C = C$-double bonds. Each point was obtained by evaluation of one single vesicle. Note that the values for DMPC, DMPC + 20 % cholesterol egg PC and C5-PC form well separated groups. The differences between the average values of K_c of adjacent groups are equal to the lowest value of K_c. Thus each group corresponds to vesicles with the same number of bilayers per cell. The lowest average K_c-values are summarized in table II. b) Structure of lipid C5-PC and G-DG.

Table I. — *Summary of average values of bending stiffness of bilayers studied in present work. Most remarkably is the low value of* K_c ($\approx 5\,kT$) *for the galactosyldiglyceride and the low value for erythrocytes.*

DMPC	: $K_c = (1.15 \pm 0.15) \times 10^{-12}$ erg
DMPC + 20 % Cholesterol	: $K_c = (2.1 \pm 0.25) \times 10^{-12}$ erg
DMPC + 30 % Cholesterol	: $K_c = (4.0 \pm 0.8) \times 10^{-12}$ erg
egg-PC	: $K_c = (1.15 \pm 0.15) \times 10^{-12}$ erg
DMPC + C5-PC 1 : 1	: $K_c = (1.7 \pm 0.2) \times 10^{-12}$ erg
G-DG	: $K_c = (1.5 - 4) \times 10^{-13}$ erg
Erythrocyte	: $K_c = (3 - 7) \times 10^{-13}$ erg

3) Most remarkably is the very low bending modulus of the digalactosyldiglyceride, that is about $K_c \approx 3\,k_B\,T$. This is partially due to the low area packing density of this lipid. Judged from accompanying monolayer studies (at the air water interface) performed in this laboratory (H.-P. Duwe doctoral thesis) the area per molecule of this lipid is by about 30 % larger (100 Å/molecule) than for DMPC (65 Å^2/molecule).

4) Another remarkable aspect is the rather low bending modulus of the red blood cell membrane. The lipid/protein bilayer of this composite membrane contains about 50 % cholesterol and 50 % of its total mass is composed of integral proteins. One would thus expect a tenfold higher value of K_c. In a forthcoming paper (K. Zeman and E. Sackmann, to be published) we will provide evidence that the bending excitations may be determined by the spectrin/actin network coupled to the bilayer.

4.2 CORRELATION TIMES OF MEMBRANE EXCITATIONS. — According to equation (4) the dynamics of each spherical harmonic mode is determined by an exponential auto-correlation function. Since the mean square amplitude of each contour excitation of wave vector q is the sum over the mean square amplitudes $|a_{\ell,m}|^2$, the auto-correlation function $\langle v_q(t)\, v_q(0)\rangle$ is also a sum over exponentials. However, it can be well approximated by a simple exponential with the decay constant (reciprocal correlation time) $\omega_q = \omega_\ell$ for the following reasons. First, the lowest order term of each sum is $q = \ell$ (cf. Eq. (8)). Second, the correlation time ω_ℓ increases approximately with the third power of ℓ and the amplitudes $a_{\ell,m}$ of the sums in equation (8) decrease with the fourth power of ℓ. The auto-correlation functions, $A_q(\tau)$, of the three lowest order modes ($q = 2$, 3 and 4) of the contour fluctuations were directly determined from the amplitudes $v_q(t)$ according to

$$A_q(\tau) = \frac{1}{S}\frac{1}{N-\tau}\sum_{n=1}^{N-\tau} v_q(t_n)\, v_q(t_{n+\tau}) \tag{14}$$

where

$$S = \frac{1}{N}\sum_n |v_q(t_n)|^2 \qquad \text{and}$$

N is the number of images evaluated for the calculation of the correlation function.

The auto-correlation functions thus determined are plotted in figure 6 for the three lowest order modes ($q = 2$, 3, 4). The experimental data can be well-fitted by a single exponential function. The oscillations of the experimental plots of $A_q(t)$ are due to experimental errors and/or slow Brownian motion of the whole vesicle during the measurement. The correlation

times of the three lowest order modes are summarized in table II and compared with values (denoted as theoretical in Tab. II) calculated from equation (5) with the measured values of K_c and the average vesicle radius r_0. For $\tilde{\gamma} = 0$ one observes a systematic discrepancy between calculated and experimental values. Good agreement is, however, observed for a value of $\tilde{\gamma} = -2.3$. This value has indeed been obtained from the static experiment by fitting the apparent value of K_c for the lowest order mode ($q = 2$) to the values obtained for $q \geqslant 3$. We thus conclude that both the dynamic and the equilibrium model of the vesicle fluctuation [7] agree well with experimental data.

Table II. — *Comparison of experimental with theoretical relaxation times* ($2\pi\tau_\ell = \omega_{\ell,m}^{-1}$) *for modes* $q = 2$ *to* $q = 4$ *as calculated for* $\gamma = 0$ *and* $\gamma = +2.3$. *Vesicle radius* $R_0 = 9.91$ μm, $K_c = 1.1 \times 10^{-12}$ erg ; *water viscosity* $\eta = 1.002$ mPs.

Relaxation time [s]	τ_2	τ_3	τ_4
theoretical : $\gamma = 0$	3.34	0.99	0.43
theoretical : $\gamma = -2.3$	2.45	0.83	0.38
experimental :	2.55	0.68	0.40

4.3 FREEZING OF UNDULATIONS AT THE L_α-$P_{\beta'}$-PHASE TRANSITION. — Figure 8 shows the temperature dependence of the mean square amplitudes of the second and third order modes in the neighbourhood of the fluid-to-solid (L_α-$P_{\beta'}$-) transition of a DMPC bilayer vesicle. Clearly, the higher order modes freeze at lower temperature than the second order excitation. Thus at decreasing temperature the mean square amplitude of the $\ell = 2$ mode starts to decrease already at 24 °C whereas that of the $\ell = 3$ mode remains essentially constant to $T = 23$ °C before reduction sets in. This is largely a consequence of the reduction of the vesicle area and the corresponding increase of the influence of the surface tension (γ). The gradual freezing of the long wavelength excitations well above the transition

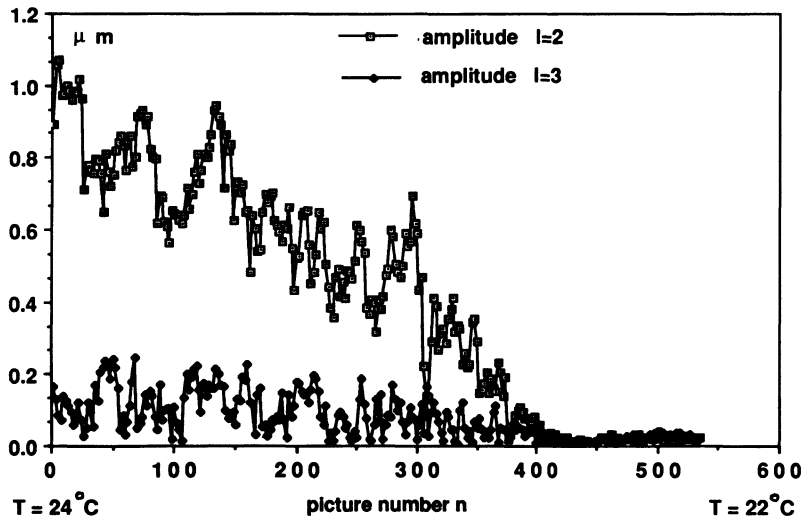

Fig. 8. — Plot of mean square amplitudes of 2nd and 3rd order modes of DMPC bilayer vesicle as a function of temperature upon approaching the fluid-to-solid phase transition. The temperature varies linearly between 24 °C at picture number $n = 0$ to 22 °C at picture number $n = 600$. The (chain) melting ($P_{\beta'}$-L_α-transition) temperature of DMPC is $T_m = 23.8$ °C.

temperature (T_m = 23.8 °C) may be the origin of the precritical behaviour of the phase transition.

4.4 HYPERELASTIC BILAYER. — An example of a drastic decrease of the membrane bending modulus by solutes is shown in figure 9. If a small amount (about 2-5 mole %) of a bipolar amphiphile (called bola lipid)

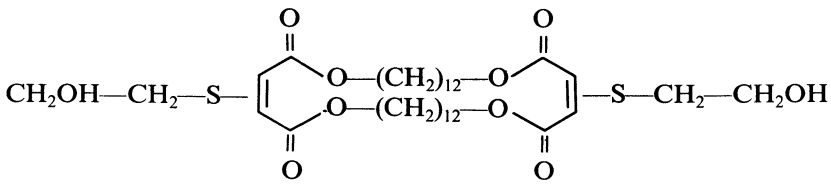

is added to DMPC, the membrane undulations are drastically enhanced. As can be seen in figure 9a, the contour is smeared which is a consequence of the very strong excitations of undulations in the sub-micrometer regime. The amplitudes of these modes are considerably larger than the half width of the contour intensity profile and a large number of these are simultaneously excited which cannot be resolved.

In addition to these fast fluctuations of the membrane, one observes slow shape changes of the vesicle which can also be seen in figure 9a (compare the first 3 pictures with the last 3). Long time observations have clearly shown that these slow shape changes are periodic.

A rough estimation shows that for a vesicle of about 10 μm radius, excitations of 5 μm wavelength (corresponding to $\ell = 5$) exhibit amplitudes of about 1 μm. This yields an approximate value of $K_c \approx 0.5\, k_B\, T$.

The very small bending stiffness and the large amplitudes of the undulations show that the DMPC-bola vesicles exhibit a very small persistence length [14]. Therefore it may be expected that these vesicles exhibit typical features of random surfaces (two-dimensional polymers) [14]. In order to explore this aspect, we determined the radius of gyration of vesicles of various size as a function of surface area at a temperature of 27 °C, that is, well above the chain-melting transition. For this purpose the coordinates of 25 points which were equidistantly distributed around the contour line of the vesicle were determined by image processing. Then the radius of gyration of the two-dimensional vesicle image was obtained according to

$$\tilde{R}_g = \left(\frac{1}{2N^2} \sum_{i=1}^{N} \sum_{j=2}^{N} R_{ij}^2 \right)^{1/2} \tag{15}$$

where R_{ij} is the distance between two points on the vesicle contour. We repeated this procedure for 10 different pictures of each vesicle evaluated. With these values of $\tilde{R}_g$, an averaged radius of gyration, R_g, was calculated. Simultaneously the surface area, A, was measured as follows : The vesicles were cooled below the L_α-P_β-transition where they assume a spherical shape which allowed the determination of A from the vesicle radius. The area, A, at the temperature of the R_g-measurement (27 °C) was obtained by assuming that the bola-containing vesicles exhibit approximately the same change in area at the phase transition ($\Delta A / A \approx 20$ %) and the same thermal expansion coefficient ($\alpha = 7.22 \times 10^{-3}$ per degree) as normal DMPC vesicles. The DMPC-bola vesicles had an average excess area of 30 % relative to the surface of a sphere of radius R_g. The relative error of our measurements was 5 % for R_g and 9 % for A.

In figure 9b the radius of gyration, R_g, is plotted as a function of the vesicle area A in a double logarithmic plot. Clearly the experimental data are well-described by a linear fit which

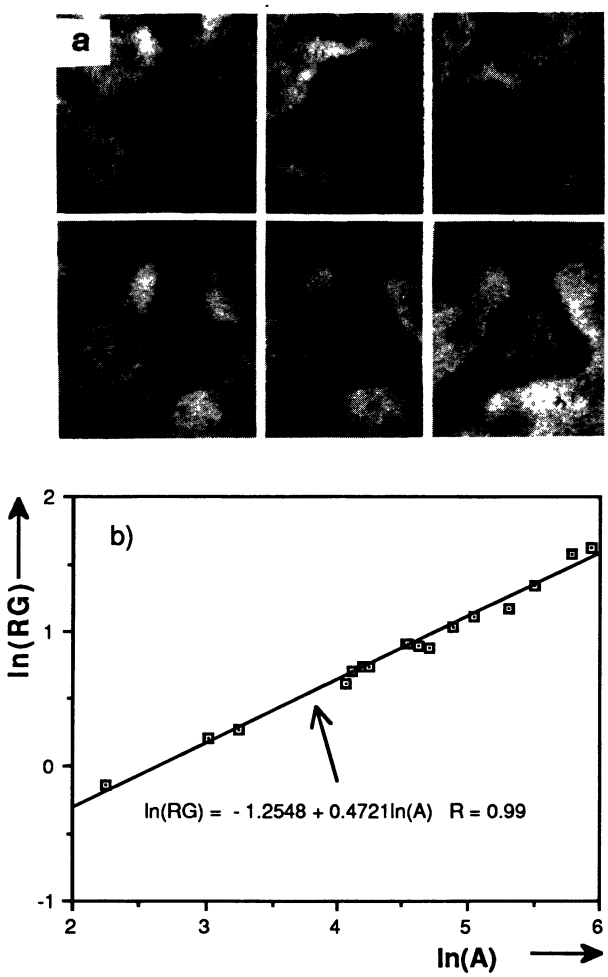

Fig. 9. — a) Transient shapes of vesicles of DMPC containing 2 mole % of the bipolar lipid denoted as bola lipid. The images were recorded from top left to bottom right. The time intervals between two images is about 10 s. The temperature was 27 °C. b) Double logarithmic plot of projected radius of gyration R_g of DMPC vesicle containing 2 mole % of the bipolar bola lipid as a function of the vesicle area A.

is confirmed by a coefficient of correlation of 0.99. From the slope of the straight line, one obtains

$$R_g^2 \propto A^{0.94 \pm 0.02}.$$

Thus R_g scales as $N^{0.94 \pm 0.02}$ where N is the number of lipid molecules.

5. Concluding discussion.

The present Fourier analysis of the shape fluctuations of vesicles allows the determination of membrane bending elastic moduli to an accuracy of 10 %. In particular, shells composed of different numbers of bilayers may be well-distinguished.

The detailed study of DMPC showed that the quasispherical model can describe the static and the dynamic aspects of the membrane excitations well. The bending mode concept

certainly breaks down at wavelengths comparable to the bilayer thickness (≈ 10 nm) where the undulations are expected to be associated with lateral tension and with shear deformations in the direction of the membrane normal [12].

The present measurements of cholesterol-containing lipid bilayers provide evidence that in this particular case, the bending mode concept breaks down even in the optical wevelengths regime. There are, of course, several reasons for the (anomalous) monotonous increase of K_c with ℓ :

(1) the decrease of thc correlation time of the undulations to values on the order of the camera integration time (0.02 s), (2) the shear associated with the mutual shift of the opposing monolayers, and (3) the lateral pressure arising in both monolayers if the lipid flow is too slow to accommodate for the local density fluctuations. At the present stage of the technique, it is not possible to distinguish unambiguously among these possibilities. Concerning the first effect, we should like to point out that we did not observe the same monotonic increase in K_c for the multilamellar vesicles, even in the case of vesicles composed of four bilayers for which K_c is increased by a factor of four. We thus favour the last effect for two reasons : first, the lateral compressibility modulus is strongly increased by cholesterol (by a factor of four at 30 mole % cholesterol, [13]) and second, the lateral mobility is substantially reduced (by a factor of about two at 30 % cholesterol).

Finally it is worth mentioning (1) that in mixed systems, one may also have a coupling between undulations and phase separation [8, 14, 15] and (2) that strong evidence has been provided that the fluid DMPC-cholesterol mixture exhibits phase separation between 10 and 30 mole % of cholesterol [16]. Thus phase separation may be another reason for the anomalous behaviour of the K_c-*versus*-ℓ plot of the DMPC-cholesterol mixture.

The remarkably low value of K_c observed for the digalactosid diglyceride is surprising in view of the fact that the area compressibility modulus reported for this lipid is similar to other common lipids [18]. The correlation between bending and area compressibility modulus suggested by micropipette experiments [17] holds well for other cases such as the cholesterol-DMPC system. On the other side, the low K_c-value for the G-DG is expected from theoretical considerations of Szleifer *et al.* [19] who showed that K_c decreases drastically with increasing surface area per molecule. As mentioned above the area per molecule for the galactolipid is by about 30 % larger than for DMPC, and a considerably lower K_c-value is thus expected. Since the bending stiffness depends also critically on the bilayer thickness [19, 20], extensive studies of bilayers of various thicknesses and packing densities are required in order to clarify this point.

Our value of $K_c = (1.15 + 0.8) \times 10^{-12}$ erg for egg lecithin is about a factor of two larger than the value reported by Faucon *et al.* [21]. Since the above value was the lowest observed by us for this lipid, we assume that it corresponds to a single shelled vesicles. We do not have an explanation for this discrepancy. On the other side, the value of the surface tension ($\gamma = 1.5 \times 10^{-5}$ erg/cm^2) reported by Faucon *et al.* agrees well with our data. Thus from $\tilde{\gamma} = 2.3$ for $r_0 = 9.9$ μm, we obtain $\gamma = 1.5 \times 10^{-5}$ erg/cm^2.

Recently, another technique for the measurement of bilayer bending stiffnesses was reported by Bo and Waugh [22]. The value obtained by these authors for stearoyl-oleyl-phosphaticlylcholine ($K_c = 2 \times 10^{-12}$ ergs) is somewhat larger than for DMPC.

In contrast to cholesterol, many small molecules lead to a reduction of the bending modulus. One example is pentanol which reduces the bending stiffness of DMPC bilayers quite drastically as shown by Safinya *et al.* [20]. This has been attributed to a thinning of the bilayer. A correlation between K_c and the thickness of the bilayer has indeed been established for the case of SDS-cosurfactant-water mixtures [20].

One striking result of the present study is the dramatic effect of a very small amount of the

bola lipid on the behaviour of DMPC vesicles. With respect to these systems the following question arises : At large excess areas (of some 10 %) vesicles may undergo a blebbing transition leading to the formation of tethers or chains of small vesicles which emanate from the giant vesicles. Such a blebbing transition has been reported by Evans *et al.* for stearoyl-oleyl phosphatidylcholine vesicles (E. Evans, private communication). In contrast, the giant DMPC-bola vesicles can assume large excess areas without blebbing. One likely explanation is that the bipolar lipid impedes the mutual sliding of the two monolayers which is required for the formation of blebs.

On the other side, DMPC vesicles with bola lipid are unstable and eventually expel small vesicles. These vesicles are completely and irreversibly separated from the giant mother vesicle and swim away. After this process the mother vesicle eventually exhibits normal shape fluctuations characteristic for DMPC. Therefore we conclude that the expelled vesicles are enriched with the bola lipid.

Our scaling law $R_g^2 \propto A^{0.94 \pm 0.02}$ establishes a fractional dimensionality of the vesicle surface. A fractional dimensionality of hyperelastic surfaces with $K_c \lesssim kT$ was predicted on the basis of Monte Carlo simulation studies by Leibler *et al.* [14] for 2-dimensional vesicles and by Baumgärtner (private communication) for the 3-dimensional case. The latter author found an exponent of 0.8. The discrepancy of the latter result with our data is most probably a consequence of the differences in the boundary conditions. For vesicles the volume V is essentially constant while in the Monte Carlo studies V is considered as variable. Another reason for the discrepancy may be attributed to the fact that we can measure only the projected radius of gyration.

A very interesting phenomenon exhibited in figure 9a is the slow and reversible transition between a more prolate and a more oblate average shape. Such slow and reversible transitions have been observed for several DMPC-bola vesicles. The response time of these slow shape changes may vary between one and some 20 minutes. These ultraslow shape fluctuations may thus correspond to the Goldstone-like modes predicted by Peterson [6] and Milner and Safran [7].

As follows from figure 5 the lamellarity of giant vesicles may be determined by K_c-measurements. In principle the lamellarity of vesicles can also be determined by optical contrast measurements [23]. However this method requires high-precision measurements of absolute contrasts if vesicles from different preparations have to be compared as in our studies. Moreover, small enclosed vesicles present in most cases may introduce large errors. For these reasons this technique was not followed further after some initial attempts. In contrast, the undulation analysis by the present technique allows absolute measurements of the lamellarity, provided the value of K_c is known.

The effect of the shear associated with the monolayer-monolayer slip depends on their coupling strength. Lateral diffusion measurements on supported bilayers [18] provide evidence for such strong coupling effects. The impeded monolayer slip certainly comes into play in the 100 nm regime as shown by the following consideration : According to equation (5) and table II, the relaxation time of the undulations is of order ℓ is $\tau_{rel} = 10 \times 10^{-3}$ s for a vesicle of $r_0 = 10$ μm, whereas the undulations wavelengths Λ scale as $\Lambda = 2\pi r_0/\ell$. On the other side, the reciprocal jump frequency of the lipid lateral Brownian motion is $\approx 10^7\ s^{-1}$. Thus the monolayer-monolayer shearing is expected to become essential for $\ell \approx 1\,500$ or for undulation wavelengths of $\lesssim 50$ nm.

Very recently we performed coherent quasielastic neutron scattering experiments of oriented multilamellar DMPC systems (at a hydration of 20 % water) by the Spin-Echo technique in the wave number regime $0.03 \lesssim q \lesssim 0.11$ Å^{-1} (W. Pfeiffer, E. Sackmann and D. Richter unpublished results). Surprisingly we find that the correlation time τ (reciprocal

line width $\omega_{\ell m}$ of the dynamic surface roughness) scales as $q^{2.5}$ to q^3, that is, similar as in the optical wavelength domain. However the value of K_c corresponding to the measured line width would be an order of magnitude smaller than expected. These short wavelength excitations may thus be of different origin.

Acknowledgements.

This manuscript was partially written during a visit at the University of British Columbia in Vancouver and one of the authors (E. S.) is most grateful to E. A. Evans for his hospitality and for many enlightening discussions. We also greatly profited from helpful discussions with W. Helfrich, S. Leibler, R. Lipowski, S. T. Milner. Last but not least, we would like to thank H. Engelhardt who pioneered the present dynamic image processing technique. The bola lipid was a gift by Prof. Furhop from the Freie Universität Berlin. The work was financially supported by the Deutsche Forschungsgemeinschaft (Project SA 246/16-2 and SFB 266 (B1)) and by the Fonds der Chemischen Industrie.

References

[1a] SACKMANN E., DUWE H. P. and PFEIFFER W., *Phys. Scr.* **T 25** (1988) 107.
[1b] ENGELHARDT H., DUWE H. P. and SACKMANN E., *J. Phys. Lett. (Paris)* **46** (1985) 395.
[1c] PETROV A. G., MITOV M. D. and DERZHANSKI A. I. in Advances of Liquid Crystal Research and Application, L. Bata Ed. (Pergamon Press Oxford) 1980.
[2] BEBLIK G., SERVUSS R. M. and HELFRICH W., *J. Phys. France* **46** (1985) 1773.
[3] BIVAS I., HANUSSE P., BOTHOREL P., LALLANE J. L. and AGUERRE-CHARIOL O., *J. Phys. France* **48** (1987) 855.
[4a] HELFRICH W., *Z. Naturforsch.* **C 28** (1973) 693.
[4b] HELFRICH W., *J. Phys. France* **47** (1986) 321.
[5] SCHNEIDER M. B., JENKINS J. T. and WEBB W. W., *J. Phys. France* **45** (1984) 1457.
[6] PETERSON M. A., *Mol. Cryst. Liq. Cryst.* **127** (1985) 257.
[7] MILNER S. T. and SAFRAN S. A., *Phys. Rev. A* **36** N° 9 (1987) 4371.
[8a] GEBHARDT C., GRULER H. and SACKMANN E., *Z. Naturforsch.* **32C** (1977) 581.
[8b] DUWE H. P., EGGL P. and SACKMANN E., *Angewandte Makromol. Chem.* **166/167** (1989) 1.
[9] BROCHARD F. and LENNON J. F., *J. Phys. France* **36** (1975) 1035.
[10] NIEDERDRENK K., « Die endliche Fourier- und Walsh Transformation mit einer Einführung in die Bildverarbeitung », Vieweg Verlag Braunschweig, 2nd ed. (1984).
[11] ZILKER A., ENGELHARDT H. and SACKMANN E., *J. Phys. France* **48** (1987) 2139.
[12] KOZLOV M. M. and MARKIN U. S., *J. chem. Soc. Farad. Trans.* **2** (1989) 85.
[13] EVANS E. A. and NEEDHAM D., *Farad. Discuss. Chem. Soc.* **81** (1986) 267.
[14] LEIBLER S., SINGH R. P. and FISHER M. E., *Phys. Rev. Lett.* **59** (1987) 1989.
[15] LEIBLER S. and ANDELMAN D., *J. Phys. France* **48** (1987) 2013.
[16] BLOOM M. and MOURITSEN O. G., *Can. J. Chem.* **60** (1988) 706.
[17] EVANS E. A. and NEEDHAM D., *J. Phys. Chem.* **91** (1987) 4219.
[18] MERKEL R., EVANS E. A. and SACKMANN E., *J. Phys. France* **50** (1989) 1535.
[19] SZLEIFER I., KRAMER D., BEN SHAUL A., ROUX D. and GELBART W. M., *Phys. Rev. Lett.* **60** (1988) 1966.
[20] SAFINYA C. R., SIROTA E. B., ROUX D. and SMITH G. S., *Phys. Rev. Lett.* **62** (1989) 1134.
[21] FAUCON J. F., MITOV M. D., MÉLÉARD P., BIVAS I. and BOTHOREL P., *J. Phys. France* **50** (1989) 2389.
[22] LIN BO and WAUGH R. E., *Biophys. J.* **55** (1989) 509.
[23] SERVUSS R. M. and BOROSKE E., *Chem. Phys. Lipids* **27** (1980) 57.
[24] PFEIFFER W., HENKEL Th., SACKMANN E., KNOLL W. and RICHTER D., *Europhys. Lett.* **8** (1989) 201.